

Non-Fraunhofer Interference Pattern in Inhomogeneous Ferromagnetic Josephson Junctions

Mohammad Alidoust,^{1,*} Granville Sewell,^{2,†} and Jacob Linder^{1,‡}

¹*Department of Physics, Norwegian University of Science and Technology, N-7491 Trondheim, Norway*

²*Mathematics Department, University of Texas El Paso, El Paso, TX 79968, USA*

(Dated: October 21, 2018)

Generic conditions are established for producing a non-Fraunhofer response of the critical supercurrent subject to an external magnetic field in ferromagnetic Josephson junctions. Employing the quasiclassical Keldysh-Usadel method, we demonstrate theoretically that an inhomogeneity in the magnitude of the energy scales in the system, including Thouless energy, exchange field and temperature gradient normal to the transport direction, influences drastically the standard Fraunhofer pattern. The exotic non-Fraunhofer response, similar to that observed in recent experiments, is described in terms of an intricate interplay between multiple '0- π '-states and is related to the appearance of proximity vortices.

PACS numbers: 74.50.+r, 74.45.+c, 74.78.FK

The well-known Fraunhofer diffraction pattern of the critical Josephson current has been extensively studied in superconductor/normal-metal/superconductor (S/N/S) junctions [1, 2]. The interest in how a supercurrent responds to an applied magnetic flux derives from the fact that this property is the key element in ultra-sensitive devices such as superconducting quantum interference devices (SQUID) [3–5]. Whereas S/N/S junctions are known to display Fraunhofer diffraction in the wide junction limit, the critical current decays monotonically as a function of the applied flux in the narrow junction limit. The crossover between these two distinct types of behavior was theoretically described in terms of proximity vortices in the normal wire [6].

More recently, the orbital response of the supercurrent in magnetic Josephson junctions has attracted much interest [3, 4]. When the normal-metal interlayer is exchanged with a ferromagnet, thus forming an S/F/S junction, a new mechanism comes into play compared to the S/N/S case. The ground-state phase difference between the superconducting reservoirs may then take the value of 0 or π , depending on parameters such as temperature and ferromagnetic barrier thickness [7]. Not only does this cause the supercurrent in magnetic Josephson junctions to decay in a non-monotonic fashion, but it was recently reported that non-Fraunhofer interference patterns appear in S/F/S junctions composed of alternating 0- and π -states [3, 4]. Whereas the supercurrent is maximal at zero flux in the non-magnetic case, the supercurrent instead displayed a minimum at zero flux in the S/F/S case [4]. These experimental findings have motivated theoretical investigations [5, 8]. Non-Fraunhofer interference patterns have also been studied in S/I/S junctions with arrays of resistors [9].

Motivated by this, the following question is answered in this Letter: under which general conditions may the critical supercurrent respond to an external magnetic field in an anomalous fashion, producing a non-Fraunhofer interference pattern? We establish these conditions and moreover explain the origin of this exotic phenomenon. To do so, we solve the quasiclassical Keldysh-Usadel equations. In the majority of past works, the investigation of the non-Fraunhofer patterns were restricted to incorporating a linear *ansatz* for the be-

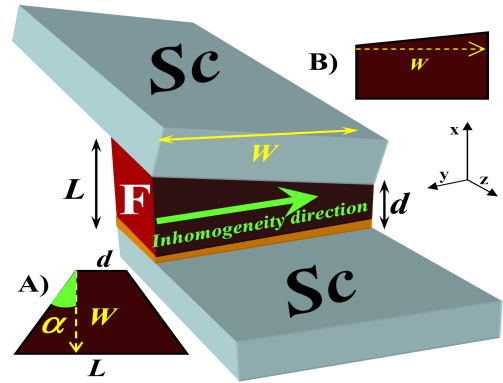


FIG. 1: Experimental setup of the inhomogeneous ferromagnetic Josephson junction. The green arrow shows the direction of the inhomogeneity in magnitude of either the Thouless energy, magnetic exchange field or temperature normal to transport direction (x -direction). To model an inhomogeneity in the Thouless energy, the setup **A**) is considered in this letter. Although making the set up **B**) might be easier to achieve technically, the two setups generate the same results in the diffusive limit. An inhomogeneity in the magnetic exchange field is modeled by $\mathbf{h} = h(0, 0, y/W)$. The external field is applied to the system in the z -direction (not shown).

havior of the superconducting U(1) phase [3, 4]. In contrast, we have employed in this Letter a model of a ferromagnetic Josephson junction which takes into account an external magnetic field with an arbitrary dependence on the coordinates and direction of the field. This model allows us to study the critical supercurrent through an inhomogeneous junction *without recourse to any ansatz*. The possibility of having an arbitrary inhomogeneous magnetization texture in the F region makes the model highly general. The results of the developed theory are qualitatively in agreement with the recent experimentally observed non-Fraunhofer patterns. Remarkably, we find that the critical Josephson current through the F region is suppressed at zero-external magnetic field within the wide junction limit when the magnitude of any of the energy scales of the system, *i.e.* Thouless energy, exchange field and temperature are inhomogeneous normal to the transport direction. Crucially, to

achieve a non-Fraunhofer response, the inhomogeneity must include at least one $0-\pi$ -state. In this case, the second peak of magnetic interference pattern of critical supercurrent becomes larger than the first, in contrast to the Fraunhofer pattern. We explain this behavior in terms of $0-\pi$ crossover states and also relate our results to the appearance of proximity vortices inside the F region.

Consider the schematic of the proposed experimental setup in Fig. 1. The inherent Josephson penetration depth λ_J is assumed to be larger than the width of junction, such that one may avoid screening effects imposed by the Josephson current on the external magnetic field. This field is assumed to be directed along the z -direction. We work with a vector potential satisfying the Lorentz gauge *i.e.* $\vec{\nabla} \cdot \mathbf{A} = 0$ and choose specifically $\mathbf{A} = -Hy\hat{x}$ in which H represents the strength of external magnetic field. The magnetic flux due to the intrinsic magnetization of the ferromagnetic region is ignored, as is known to be a good approximation in most cases [4]. To investigate the transport properties of this system, the quasi-classical theory of superconductivity in the diffusive regime is employed, so that the Gor'kov equations are reduced to the Usadel equations [10]. The Usadel equation inside the F region together with appropriate boundary conditions is used for obtaining observable quantities of the system. In the presence of a static external magnetic field, the Usadel equation is succinctly given by;

$$D[\hat{\partial}, \check{\mathbf{g}}(x, y, z)[\hat{\partial}, \check{\mathbf{g}}(x, y, z)]] + i[\varepsilon\hat{\rho}_3 + \text{diag}[\mathbf{h}(x, y, z) \cdot \underline{\sigma}, (\mathbf{h}(x, y, z) \cdot \underline{\sigma})^T], \check{\mathbf{g}}(x, y, z)] = 0, (1)$$

where $\mathbf{h}(x, y, z)$ stands for exchange energy, $\check{\mathbf{g}}$ is the full 8×8 Green's function matrix, while $\hat{\rho}_3$ and $\underline{\sigma}$ are 4×4 and 2×2 Pauli matrixes, respectively [18]. Here D is the diffusion constant and $\hat{\partial} \equiv \vec{\nabla} \hat{1} - ie\mathbf{A}(x, y, z)\hat{\rho}_3$. Within the weak proximity regime, one may can expand the Green function around the bulk solution $\hat{\mathbf{g}}_0$ *i.e.* $\check{\mathbf{g}}(x, y, z) \simeq \hat{\mathbf{g}}_0 + \hat{f}(x, y, z)$, where $\hat{\mathbf{g}}_0 = \text{diag}(\underline{1}, -\underline{1})$ [11]. Therefore, the retarded component of Green's function reads:

$$\hat{\mathbf{g}}^R(x, y, z) \approx \begin{pmatrix} \underline{1} & \underline{f}^R(x, y, z) \\ -\underline{f}^R(x, y, z) & -\underline{1} \end{pmatrix}. (2)$$

The advanced and Keldysh blocks are also given via $\hat{\mathbf{g}}^A(x, y, z) = (\hat{\rho}_3 \hat{\mathbf{g}}^R(x, y, z) \hat{\rho}_3)^\dagger$ and $\hat{\mathbf{g}}^K(x, y, z) = (\hat{\mathbf{g}}^R(x, y, z) - \hat{\mathbf{g}}^A(x, y, z)) \tanh(\varepsilon/2k_B T)$ under equilibrium conditions. At the two N/S interfaces the Kupriyanov-Lukichev boundary conditions [12] are compactly written by: $2\zeta \hat{\mathbf{g}}[(\vec{\nabla} - ie\mathbf{A}\hat{\rho}_3) \cdot \hat{n}, \hat{\mathbf{g}}] = [\hat{\mathbf{g}}_{\text{BCS}}(\phi), \hat{\mathbf{g}}]$, the ratio between the resistance of the barrier region and the resistance in the F film is defined as $\zeta = R_B/R_F$, $\hat{\mathbf{g}}_{\text{BCS}}(\phi)$ is the Green's function in the two superconductor reservoirs [13] and \hat{n} is a unit vector normal to the interface [11]. At the vacuum borders, the Green's function satisfies $\partial_y \hat{\mathbf{g}} = 0$.

The Usadel equations in their present form constitute a set of complicated coupled differential equations which we have solved numerically by using a collocation method. Thus,

the approximate solution components are assumed to be linear combinations of bicubic (tricubic, for three-dimensional problems) Hermite basis functions, and required to satisfy the Usadel equation exactly at 4 (8, for three-dimensional problems) collocation points in each subrectangle of a grid, and to satisfy the boundary conditions exactly at certain boundary collocation points [14]. Finally, Newton's method is used to solve the (nonlinear, generally) algebraic equations resulting from the collocation method formulation [17]. In order to study transport properties of the inhomogeneous junction, the current density through the junction is considered: $\mathbf{J}(\vec{R}, \phi) = J_0 \int d\varepsilon \text{Tr}\{\rho_3(\check{\mathbf{g}}[\hat{\partial}, \check{\mathbf{g}}])^K\}$, here $J_0 = N_0 e D / 4$ and N_0 is the number of states in the Fermi surface. Performing an integration over the y -coordinate provides the total supercurrent flowing through the junction, $I(\phi) = I_0 \int \int dy d\varepsilon \text{Tr}\{\rho_3(\check{\mathbf{g}}[\hat{\partial}, \check{\mathbf{g}}])^K\}$. To understand the magnetic interference patterns of such junctions, we also investigate the spatial variation of pair potential inside the F region calculated via: $U = U_0 \text{Tr}\{(\hat{\rho}_1 - i\hat{\rho}_2) \int d\varepsilon \hat{\tau}_3 \check{\mathbf{g}}^K\}$, where $U_0 = -N_0 \lambda / 16$ [18]. The temperature, width and lower base of the *wedged* junction are fixed at $T/T_c = 0.01$, $W/\xi_S = 10$ and $d/\xi_S = 2$, respectively (the so-called wide junction limit). The proximity controlling parameter ζ is also fixed at 5, ensuring that we operate in the weak proximity regime. Energy units are used so that $\hbar = k_B = 1$.

The results for the critical Josephson current through the inhomogeneous S/F/S junction as a function of normalized external magnetic flux *i.e.* Φ/Φ_0 are presented in Fig. 2. In frame **A**), the magnitude of the Thouless energy is inhomogeneous in the y -direction: the F region has a wedged shape [see **A**] in Fig. 1]. In frame **B**), the magnitude of magnetic exchange interaction is inhomogeneous in the y -directions and follows a $\mathbf{h} = \mathbf{h}(0, 0, y/W)$ pattern. The normalized critical current I_c/I_0 exhibits a suppression at zero external flux for some values of the wedge angle α . In the case of trapezoidal junction, the second peak in the interference pattern takes a larger value than the first for an interval of α -values. Typically, this behavior is enhanced at $\alpha = \pi/43$ and then disappears for larger values $\alpha > \pi/20$ (see inset panel of panel **A**) of Fig. 2). A similar magnetic interference pattern is generated when the magnitude of exchange field is inhomogeneous, as shown in frame **B**). In this case, the non-Fraunhofer pattern phenomenon is pronounced for *e.g.* $h = 4.27\Delta$. The results show qualitatively good consistency with recently reported non-Fraunhofer patterns for " $0-\pi$ "-stacks in Ref. 4. For reasons to be described below, we expect that the same non-Fraunhofer magnetic pattern would arise when the temperature of the system along the y -direction is variable and has an inhomogeneous form. We have also investigated (not shown) other magnetization textures such as domain-wall, skyrmion and spiral (with helical axis normal to transport direction), and found that they generate the standard Fraunhofer patterns because of the constant magnitude of the magnetic exchange field, $|\mathbf{h}| = h$.

In comparison, the behavior of critical Josephson current through a S/N/S wedged junction is investigated in Fig. 2 C).

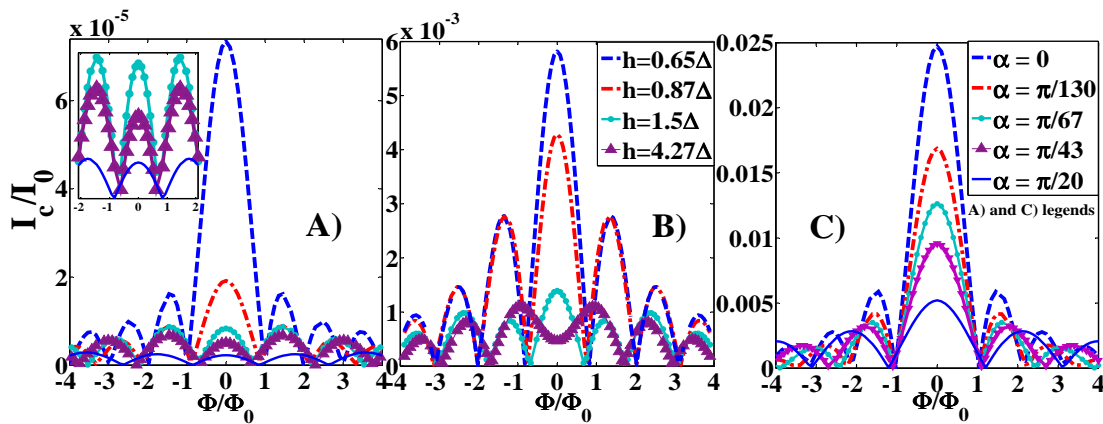


FIG. 2: Normalized supercurrent through an inhomogeneous Josephson junction vs normalized external magnetic flux Φ/Φ_0 perpendicular to the junction. **A)** An S/F/S junction where the F region has a wedged shape with inclination angle α and exchange field $h = 10\Delta_0$. The inset panel zooms in on the interference pattern at small and large values of Φ and α , respectively. **B)** The F region is now geometrically rectangular, but the magnitude of exchange field is now inhomogeneous according to the texture $\mathbf{h} = h(0, 0, y/W)$. **C)** An S/N/S junction where the N region has a wedged shape with inclination angle α . The legends are the same as in **A)**. In all cases, the height of the trapezoidal region is fixed at $W = 10\xi_S$ while the upper base d is equal to $2\xi_S$ (see Fig. 1). Therefore, $\alpha=0$ makes a rectangular junction ($L = d = 2\xi_S$) and $\pi/130$ ($L = 2.483\xi_S$), $\pi/67$ ($L = 2.938\xi_S$), $\pi/43$ ($L = 3.463\xi_S$) and $\pi/20$ ($L = 5.168\xi_S$) make wedged junctions.

For $\alpha = 0$, we recover the results of Ref. 6. With increasing α , the normalized supercurrent is subject to an overall reduction, because the effective junction length increases due to the inhomogeneity in the magnitude of Thouless energy. Unlike the inhomogeneous S/F/S case above, however, the first peak in the diffraction pattern is larger than others for all values of α , exhibiting the standard Fraunhofer pattern. Therefore, the exotic non-Fraunhofer pattern only can be observed in ferromagnetic junctions under the conditions discussed above.

To further understand the outstanding difference between interference patterns of the homogeneous and inhomogeneous ferromagnetic junctions, we consider how the presence of an external magnetic field influences both the $0-\pi$ transition profile of the S/F/S junction and the proximity vortices pattern in the F region. The origin of the suppressed central peak in the S/F/S wedged Josephson junction ($\alpha \neq 0$) is mainly studied in this Letter, and we argue why this mechanism accounts for the non-Fraunhofer pattern in other cases where there is a magnitude gradient of the exchange field and/or temperature along the direction normal to the transport direction so that it includes at least one $0-\pi$ -state. To this end, we will later investigate the current density spatial map of magnetic junctions and compare $\alpha=0$ with $\alpha \neq 0$. Fig. 3 reveals an illustrative profile of the normal and ferromagnetic Josephson junctions. Part **A)** illustrates a spatial map of pair potential in the normal region of the S/N/S junction where $\alpha=0$ and $\pi/43$ for the left and right panels, respectively. The upper base of the trapezoidal region is fixed at $d = 2\xi_S$ while for $\alpha=\pi/43$ the lower base takes the value $L=3.463\xi_S$. The increment of α deforms the proximity vortex pattern compared to the pattern of the rectangular junction. The distance between two neighboring vortices is no longer equal to $\Phi_0 H/d$ in contrast to that of rectangular junction within the wide junction regime (left panel). The spatial maps of the pair potential are given for $\Phi=4\Phi_0$

and zero superconducting phase difference *i.e.* $\phi=0$. Now, the increment of α removes the proximity vortices inside the normal segment of the junction gradually. The variation of superconducting phase difference ϕ however, moves the vortices along the \hat{y} -direction in both the normal and ferromagnetic junctions [6]. Part **B)** exhibits the equivalent investigation for a ferromagnetic Josephson junction. In the rectangular case, the pair potential shows the same behavior as the vortex pattern as S/N/S case. In contrast, the vortex pattern is highly deformed in the wedged ferromagnetic junction. A zoom-in is shown for the middle of F wire with $\alpha=\pi/43$ using different color map. The strong deformation may be understood by noting that the increment of α effectively synthesizes multiple " $0-\pi$ " states in the same junction and also from the pair-breaking of the exchange field. When α becomes non-zero, the junction may be thought of as a superposition of multiple 0 and π junctions.

To understand this quantitatively, parts **C)** and **D)** should be considered together. Part **C)** illustrates the $0-\pi$ crossover profile where $\alpha = 0$ for two different values of external flux $\Phi=0, 3\Phi_0/2$ as a function of F-layer length d/ξ_S . The first and second transitions occur at $d=2.38\xi_S$ and $3.46\xi_S$, respectively. It is important to note that the latter length is identical to the lower base of the trapezoidal junction when $\alpha=\pi/43$. The plot also shows that applying an external magnetic field reduces the magnitude of the current nonlinearly, although the locations of $0-\pi$ points are left unchanged. The anomalous Fraunhofer diffraction pattern of the critical supercurrent can now be well understood by noting part **D)**. Increasing the junction angle α renders more parts of the junction to have opposite supercurrent flow direction which then partially cancel each other. One should note that in the trapezoidal region, the amplitude of critical current is non-uniform. More π -parts, therefore, are needed to cancel the 0 -parts of the junction that

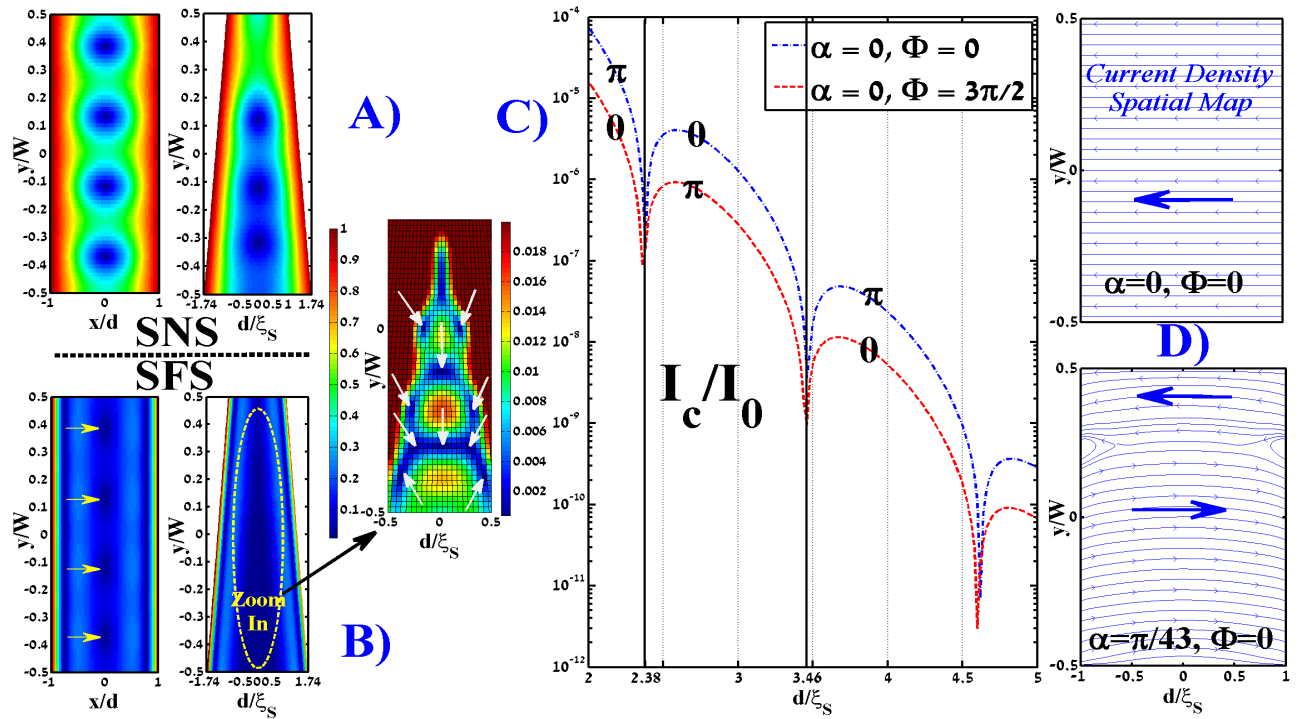


FIG. 3: **A)** Normalized spatial map of the pair potential for a S/N/S junction where $\alpha=0, \pi/43$ ($L=3.463\xi_S$) in the left and right frames, respectively. **B)** The normalized pair potential in a S/F/S junction. Arrows indicate the location of proximity vortices. The zoom-in frame of a S/F/S trapezoidal junction with $\alpha=\pi/43$ is shown using a different color map. The magnetic flux through the N or F region is assumed to be $\Phi=4\Phi_0$ and no superconducting phase difference is applied ($\phi=0$). **C)** The $0-\pi$ crossover profile of a rectangular S/F/S junction where $\Phi=0, 3\Phi_0/2$ and $W = 10\xi_S$ vs. normalized junction length d/ξ_S . **D)** Current density spatial map of the magnetic Josephson junction in the absence of external magnetic field, $\Phi=0$. Top and bottom frames exhibit current density flowing through the junction where $\alpha=0, \pi/43$, respectively ($\alpha=\pi/43$ constitutes a '0- π '-junction). Blue arrows indicate current directions.

occur for the top region with smallest effective length L . A key observation is that the above results suggest a venue for producing an anomalous non-Fraunhofer interference pattern resulting without necessarily distorting the geometry of the system, in effect allowing for anomalous interference even in standard rectangular junctions.

In conclusion, we have proposed experimentally accessible generic conditions for achieving non-Fraunhofer interference patterns of the critical supercurrent as a function of external magnetic flux. The key property is the controllable numbers of gradual $0-\pi$ states in the same junction by incorporating an inhomogeneity in the magnitude of energy scales of system *i.e.* Thouless energy, exchange field and/or temperature normal to the transport direction. We examine the proposed generic conditions for some limiting cases and find good qualitative consistency with the recently observed non-Fraunhofer magnetic interference patterns in $0-\pi$ stacks.

The authors are grateful to F. S. Bergeret and J. W. A. Robinson for valuable discussions, and thank A. Sudbø for conversations during the initial stages of this work and K. Halterman for his generosity regarding compiler source.

* Electronic address: phymalidoust@gmail.com

† Electronic address: sewell@utep.edu

‡ Electronic address: jacob.linder@ntnu.no

- [1] J.M. Rowell, *Phys. Rev. Lett.* **11**, 200 (1963); J. Clarke, *Proc. R. Soc. A* **308**, 447 (1969); S. Nagata *et al.*, *Phys. Rev. B* **25**, 6012 (1982); H. C. Yang *et al.*, *Phys. Rev. B* **30**, 1260 (1984); G. Mohammadkhani *et al.*, *Phys. Rev. B* **77**, 014520 (2008).
- [2] J. P. Heida *et al.*, *Phys. Rev. B* **57**, 5618 (1998); V. Barzykin *et al.*, *Superlatt. and Microstruct.* **25**, 797 (1999); U. Leder mann *et al.*, *Phys. Rev. B* **59**, 9027 (1999).
- [3] S. M. Frolov *et al.*, *Phys. Rev. B* **74**, 020503(R) (2006).
- [4] M. Weides *et al.*, *Phys. Rev. Lett.* **97**, 247001 (2006); M. Kemmler *et al.*, *Phys. Rev. B* **81**, 054522 (2010); C. Gurlich *et al.*, *Phys. Rev. B* **81**, 094502 (2010).
- [5] N. G. Pugach *et al.*, *Phys. Rev. B* **80**, 134516 (2009).
- [6] L. Angers *et al.*, *Phys. Rev. B* **77**, 165408 (2008); J. C. Cuevas *et al.*, *Phys. Rev. Lett.* **99**, 217002 (2007); F. S. Bergeret *et al.*, *J Low Temp Phys* **153**, 304 (2008).
- [7] V. V. Ryazanov *et al.*, *Phys. Rev. Lett.* **86**, 2427 (2001); T. Kontos *et al.*, *Phys. Rev. Lett.* **89**, 137007 (2002); J. J. A. Baselmans *et al.*, *Nature (London)* **397**, 43 (1999); J. Huang *et al.*, *Phys. Rev. B* **66**, 020507(R) (2002).
- [8] E. Goldobin *et al.*, [arXiv:1110.2326](https://arxiv.org/abs/1110.2326).
- [9] M. A. Itzler *et al.*, *Phys. Rev. B* **51**, 435 (1995).
- [10] K. D. Usadel, *Phys. Rev. Lett.* **25**, 507 (1970); A. I. Larkin and Y.

- N. Ovchinnikov, in *Nonequilibrium Superconductivity*, edited by D. Langenberg and A. Larkin (Elsevier, Amsterdam, 1986), P. 493.
- [11] F. S. Bergeret *et al.*, *Rev. Mod. Phys.* **77**, 1321 (2005); F. S. Bergeret *et al.*, *Phys. Rev. Lett.* **86**, 3140 (2001).
- [12] A. V. Zaitsev, *Zh. Eksp. Teor. Fiz.* **86**, 1742 (1984) (*Sov. Phys. JETP* **59**, 1015 (1984)); M. Y. Kuprianov *et al.*, *Sov. Phys. JETP* **67**, 1163 (1988).
- [13] J. Linder *et al.*, *Phys. Rev. B* **77**, 174514 (2008); M. Alidoust *et al.*, *Phys. Rev. B* **81**, 014512 (2010).
- [14] Although the collocation method seems to be applicable only to rectangular regions, it can actually be used to easily solve problems in a wide range of simple two-dimensional and three-dimensional regions, as is outlined in Ref. 16.
- [15] G. Sewell, *The Numerical Solution of Ordinary and Partial Differential Equations, second edition*, John Wiley & Sons, (2005);
- [16] G. Sewell, *Advances in Engineering Software* **41**, Iss. 5, 748-753 (2010).
- [17] The iterative solver which we used is a “Jacobi” conjugate-gradient method, which means that the conjugate gradient method (Section 4.8 of Ref. 15) is applied to the preconditioned equations $D^{-1}A^T A \mathbf{x} = D^{-1}A^T \mathbf{b}$, where D is the diagonal part of $A^T A$.
- [18] J. P. Morten, M.Sc. thesis, Norwegian University of Science and Technology (2003).